International Journal of Chemical and Biochemical Sciences
(ISSN 2226-9614)

Journal Home page: www.iscientific.org/Journal.html

Development of reusable Iron Sulfide nanoparticles *via* hydrothermal route for Photocatalytic degradation of 2,4-Dinitrophenol

***D. Aditya Deepthi*[a, *], *B. Sathish Mohan*[b,*]**

[a]*Dept. of Chemistry, St. Joseph's College for Women (A), Visakhapatnam, India*

[b]*Bio Enviro Chemical Solutions, Visakhapatnam, India*

Abstract

Dye impurities are the very hazardous parameters that contaminate water and cause significant health problems. The dye 2,4-DiNitroPhenol (2,4-DNP) causes eye and skin annoyance, nausea, diarrhea, intestinal pain, and vomiting. As a result, there is a need to progress a low-cost, simple, and effective photocatalyst for the degradation of 2,4-DNP dye from polluted water. The fabrication of iron sulphide (FeS_2) *via* a simple, straight forward hydrothermal route is stated in this study. This metal sulphide contributes new, hybrid, and effective properties to increased catalytic action. XRD patterns, SEM EDX, FTIR, UV-VIS Spectroscopy and XPS analysis, on the other hand, confirmed the formation of desirable iron sulphide. A basic 2,4-DNP was 74% decolored in 90 minutes by characterized FeS_2 with 50 mg. This is demonstrated by the addition of FeS_2 (35 nm), resulting in a higher photocatalytic activity. As a result, this research encourages the development of extra effective heterostructures for improved photocatalytic act.

Keywords: FeS_2, Photocatalysis, Hydrothermal, 2,4-DiNitroPhenol

Full length article **Corresponding Author*, e-mail: dadityadeepthi@stjosephsvizag.com

1. Introduction

Millions of tons of dye have been produced in recent years and settled into water resources without any purification or treatment [1]. Around 15% of dyes are lost during production and released as textile effluents [2]. As a result, waste-water handling is a essential step in dye elimination. Recent waste-water treatment studies provide a variety of dye removal methods, including physical methods such as biodegradation [3], adsorption [4], ozonationand chlorination [5]. Despite their advantages, these methods are not widely used due to processing and economic constraints. A sophisticated oxidation procedure for water treatment has recently been developed. The generation of reactive free radicals is used in this method to degrade dyes from waste water. Photocatalytic water treatment processes have numerous advantages, including full mineralization of organic pollutants and dyes dissolved and dispersed in water, low cost, and a high rate of response [6]. As a result, photocatalytic degradation of organic pollutants has received a lot of attention [7-10]. The development of abundant visible light-active materials is critical for their technological integration into environmental and energy-related processes. The main applications are photocatalytic hydrogen evolution, carbon dioxide reduction, and organic compound breakdown in water [11, 12]. Metal sulfides have piqued the interest of researchers due to their potential for optical and electrical applications [13]. Sulfide photocatalysts such as CdS, ZnS, FeS_2, CuS, NiS_2, and MoS_2 have received the most attention due to their band gap energy matching the solar spectrum [14,15]. One of them is FeS_2, also known as pyrite. Its intriguing electronic and optical properties, combined with its environmental friendliness, high photo-absorption in the visible portion of the solar spectrum, and high absorption in the visible portion of the solar spectrum, make it an additional promising candidate for photosensitization of materials. In our research, we created iron (II) sulfide (FeS_2), which is cheap, stable, nontoxic, and widely available. Organic dyes such as methylene blue, rhodamine B and methyl orange [16], rose bengal [17], reactive black & reactive orange [18], and phenol [19] can be efficiently adsorbent and photo catalytically degraded by it because of its surface chemical properties, high optical absorption coefficient (6x105 cm-1) [20], high capacity (exceeding 890 mA h g-1), and appropriate band gap (1.00 0.15 eV [21]. Because of these intriguing properties, FeS2 has been studied for use in solar devices [22] and lithium-ion batteries [23]. As previously reported [24], FeS2 can be produced using a variety of methods, including hydrothermal, solvothermal, metal organic chemical vapor deposition, and sulfurization of iron or iron oxide films. Di Nitro Phenol (DNP) has numerous

applications in agriculture as a pesticide and in the petrochemical industry as a polymerization inhibitor for vinyl aromatics, but it is carcinogenic and toxic when used in excess, so the US Environmental Protection Agency (EPA) has restricted and declared that a cost-effective and efficient method for removing DNP from contaminated water is required [25, 26]. According to researchers, photocatalysis is an effective method for removing organic dye pollutants [27]. However, semiconductor nanoparticles have demonstrated excellent photocatalytic performance due to their low cost, optical, electrical, and biochemical properties, as well as a wider bandgap that captures solar light and the ability to ruggedize in visible light active. As a result, the synthesis of iron sulphide via a hydrothermal route has been reported in this work, and their chemical properties have been further studied using sophisticated instruments. Using visible light irradiations, the photocatalytic activity of the prepared composite was measured over Dinitrophenol (DNP).

2. Methods

Sigma Aldrich Company, India, provided sodium sulfide (Na_2S), ferric chloride ($FeCl_3$), and sodium borohydride ($NaBH_4$), which were used without extra decontamination. Nitrophenol was obtained from Merck Chemical Ltd in India and used without extra decontamination, while Milli Q water was used in all preparation solutions. The requisite FeS_2 was obtained in this investigation using the hydrothermal technique. Simply said, equal volumes (10 mL) of Na_2S (0.05M) and FeCl3 (0.01M) were combined in a beaker and rapidly stirred for a duration of one hour. This blended solution was given a pinch of $NaBH_4$ and swirled for an hour. After quickly transferring the combined solution into a hydrothermal beaker and sealing it, it was heated to 180ºC for 12 hours in a furnace. Following the completion of the reaction, the mixed solution was cooled to room temperature and repeatedly cleaned with water and ethanol. Ultimately, the resultant product underwent filtration and was allowed to dry for an entire night at 70ºC in a hot air stabilizer.

2.1 Instrumentation

The produced catalysts were further thoroughly examined with analytical tools, and morphology and elemental composition were examined under a SEM microscope through EDX analysis. With a Cu-kα wavelength and a scan rate speed of 0.02ºC, the Bruker AXS D8 Advance X-ray diffractometer was used to analyze the compound's crystallinity utilizing XRD patterns. XPS (PHI 5000 versa probe III) and UV-visible spectrophotometer (Shimadzu 2600R) were used to examine the optical properties of prepared samples in the wavelength range of 200-800 nm. FTIR analysis (IR prestige 21, Shimadzu) was used to determine the functional groups on the catalyst surface in the range of 500 to 4000 cm-1.

2.2 Photocatalytic performance

Under visible light illumination, the photocatalytic activity of produced FeS_2 was investigated for the breakdown of the organic contaminant 2,4-DNP. According to published research, the FeS_2 was first subjected to harsh testing conditions, including 0.05 g of catalyst and 10 ppm of an alkaline 2,4-DNP solution. Every reaction was carried out under standard air pressure and at ambient temperature. 50 mL of 2,4-DNP solution included 50 milligrams of the catalyst suspended in it. The system was magnetically agitated for 30 minutes prior to irradiation in a completely dark atmosphere until adsorption-desorption equilibrium was attained. Following this, the system was exposed to visible light, which triggered the photocatalytic activity. The catalyst was removed from the mixed solution by centrifuging 4-5 mL of it at regular intervals. The dye's concentration was measured using a UV-Vis spectrophotometer.

Equation (1) was used to determine the photocatalytic reaction's degradation efficiency.

$$\text{Degradation efficiency (DE\%)} = \frac{C_0 - C_t}{C_0} \times 100 \longrightarrow (1)$$

where "Ct" is the concentration or absorbance following the photocatalytic reaction at different times "t," and "C0" is the initial concentration or absorbance.

3. Results and Discussion

3.1 X-Ray diffraction analysis

Figure 1 shows the X-ray powder diffraction patterns of the synthesized FeS_2. FeS_2 showing the XRD patterns as 15.5º, 18.3º, 25.8º, 30.5º, 35.3º, 40.1º, 46.2º, 51.3º, 56.2ºand 60.5º (JCPDS: 01-079- 0617). Noticed that few peaks were seen beyond 30º, confirms there are no peaks of FeS, means the formation of FeS_2. The average particles size of prepared FeS_2 nanoparticles was estimated by Debey-Scherrer's formula and found that it was 35 nm.

3.2 Fourier Transform Infrared analysis

The FTIR spectrum of FeS_2 produced by the hydrothermal method is shown in Fig. 2. Functional groups of Fe=S, Fe–S, and S–S were demonstrated in the samples by FTIR spectra. The VIBration modes of disulfide (S-S) and Iron sulphide (Fe–S) existed at 612 Cm^{-1} and 1100 Cm^{-1} respectively [28]. FeS_2's FTIR spectra showed peaks at 3374 cm-1, which indicates that water molecules contain O-H stretch vibrations.

3.3 UV- Visible spectroscopy analysis

Ensuring that the particles are evenly distributed throughout the solution is crucial in this situation. If nothing else, they shouldn't precipitate to the bottom before the metallic nanostructures are added, but a well-dispersed solution is essential for the best outcome. In this connection, the UV-Vis absorbance spectrum of FeS_2 NPs is reported as Fig. 3 which consists of a broad band having maximum at around 230 nm followed by other peaks at 358 and 436 nm.

3.4 Scanning electron microscopy study

Fig. 4 (a-c) displays the SEM and EDX analysis of prepared FeS_2 sample The morphological investigation reveals that the as-prepared FeS_2 is composed of particle agglomerates. Polyhedral particles of 35 nm are detected in the FeS_2 sample. Using Image J software to count 300 particles, these figures show the average particle size. A regulated growth during the hydrothermal synthesis is responsible for the consistent shape and particle size distribution seen in all of the samples.

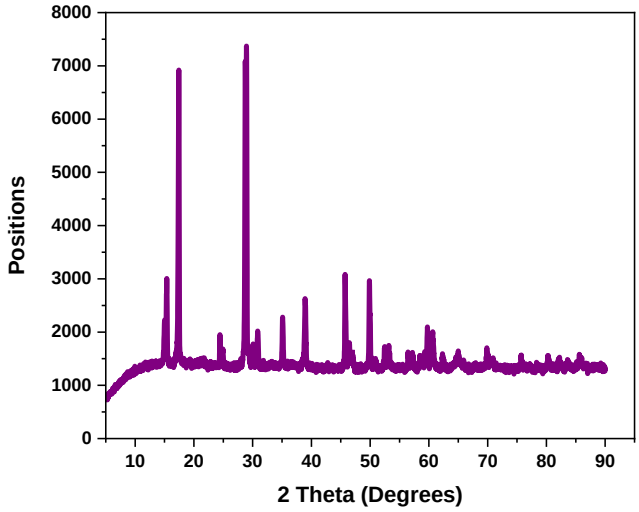

Figure 1: XRD Patterns of prepared material FeS_2

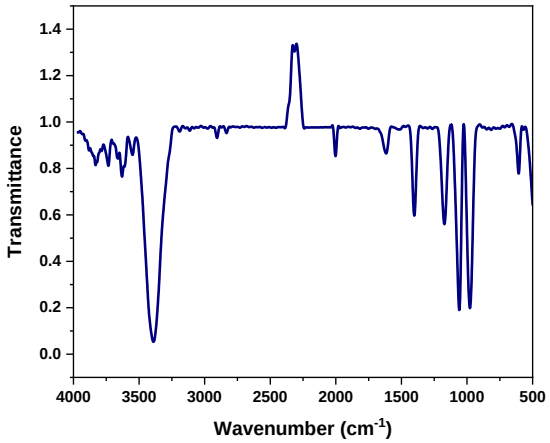

Figure 2: FTIR Spectrum of prepared material FeS_2

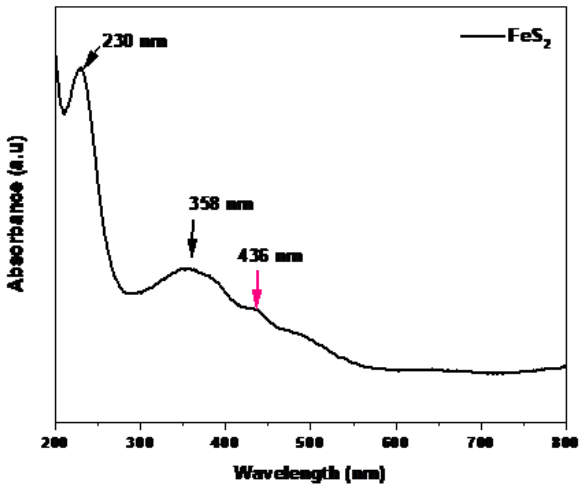

Figure 3: UV- Visible absorption spectra of FeS_2

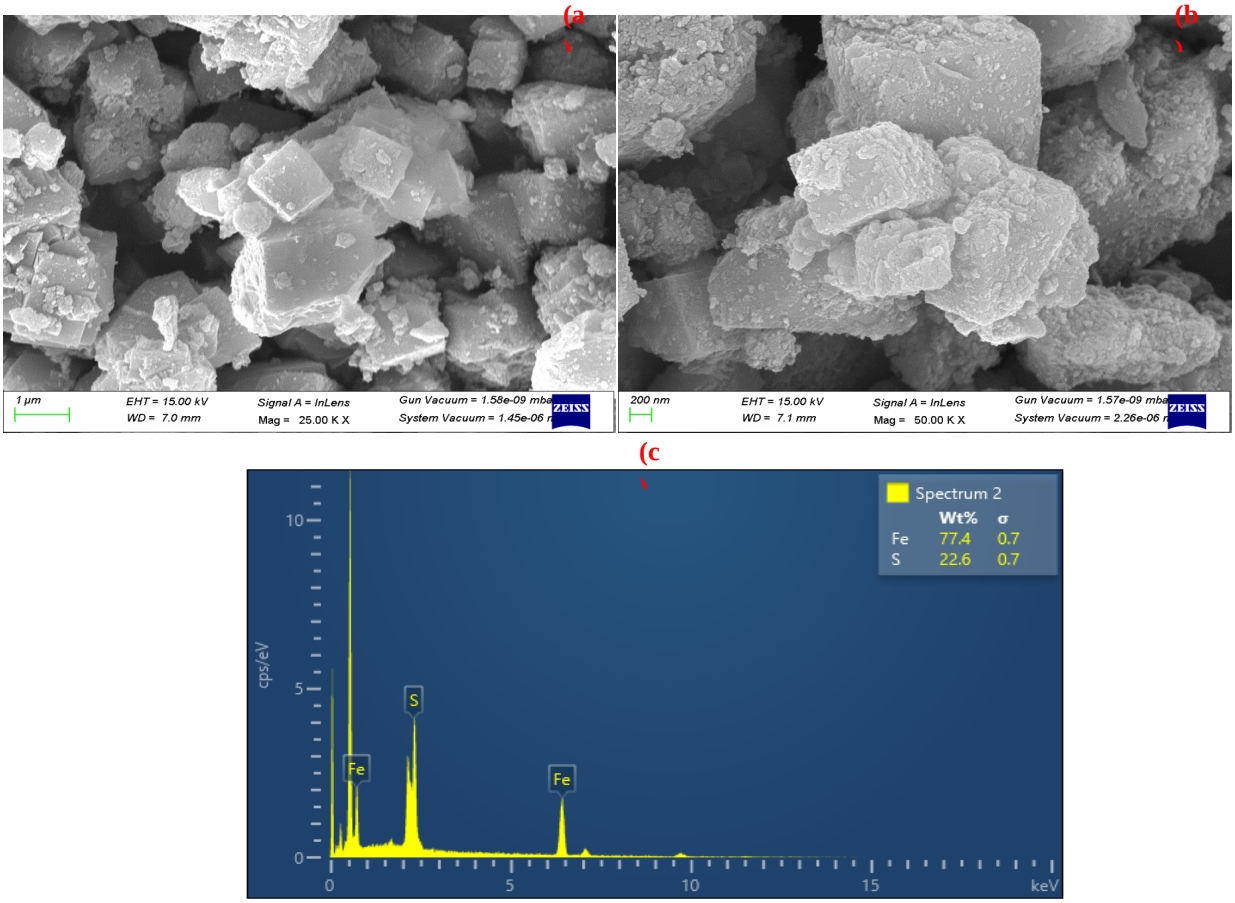

Figure 4: (a-b) SEM and (c) EDX analysis of prepared FeS_2

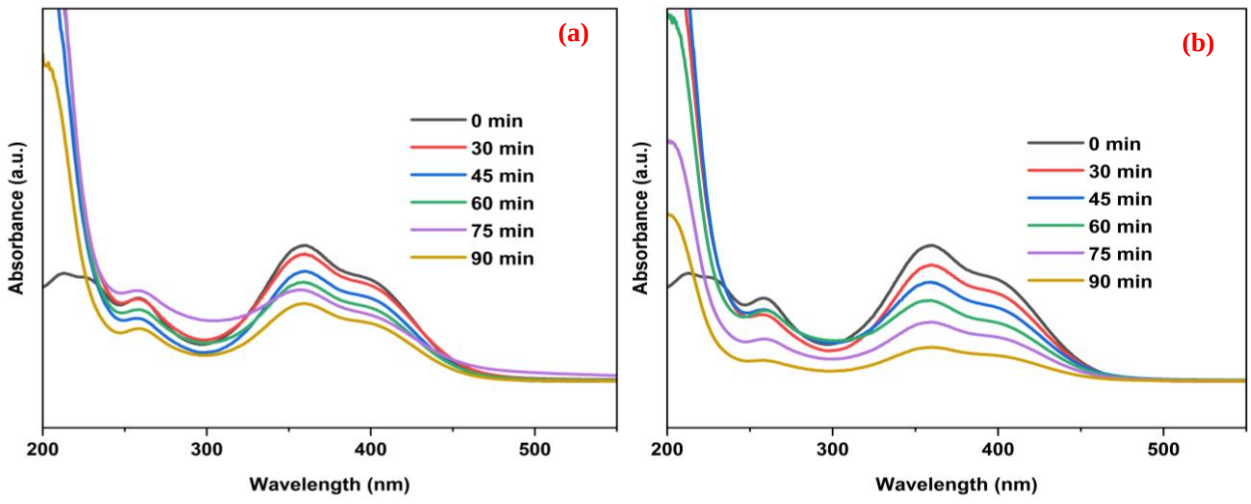

Fig 5: XPS spectral analysis of prepared FeS_2

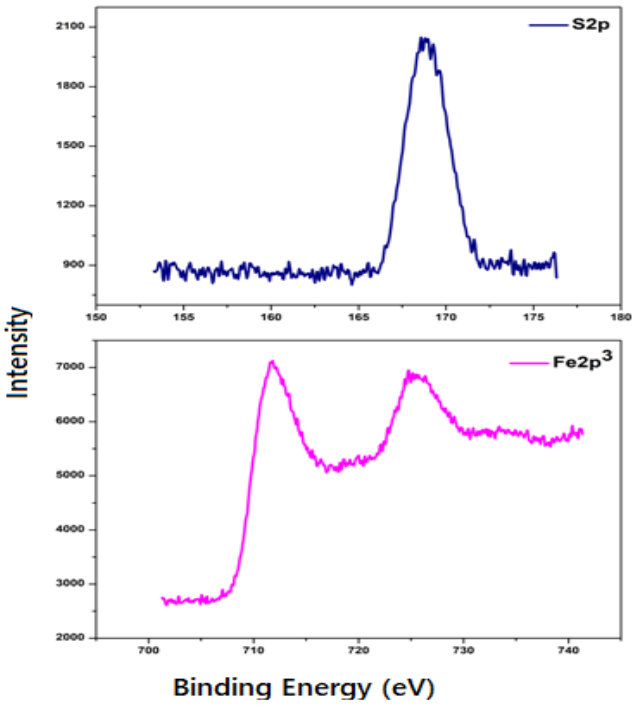

Fig 6: Photocatalytic degradation of 2,4-DNP using (a) Commercialized and (b) Prepared FeS_2

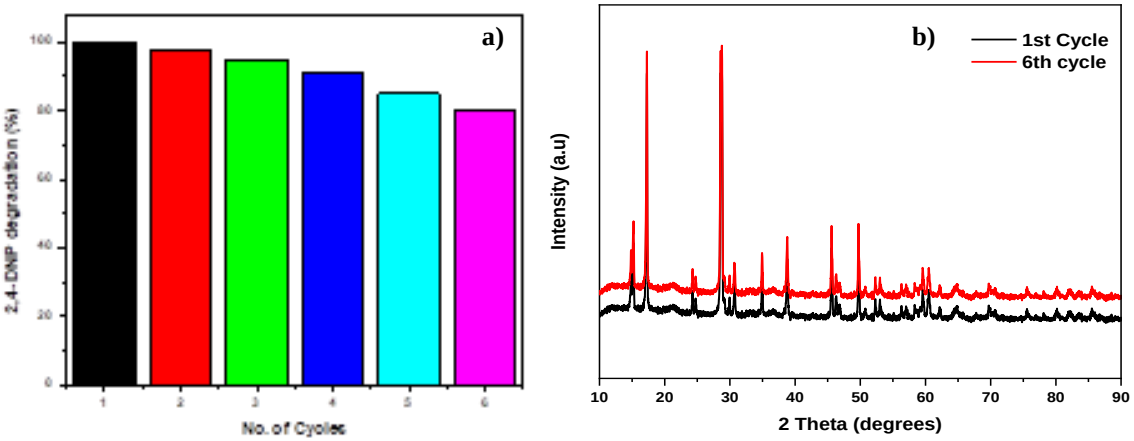

Fig 7: Recyclability (a) and Sustainability (b) of prepared FeS_2

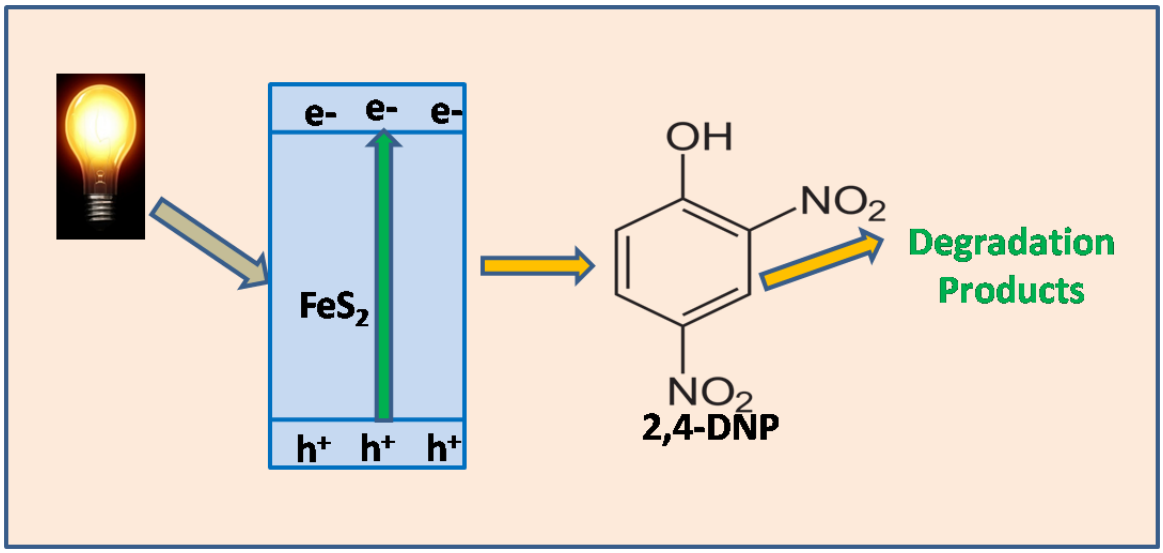

Fig 8: Possible mechanism for degradation of 2,4-DNP using FeS_2

Small particle sizes are advantageous to the photocatalytic process because they enable the photogenerated charges to go from the bulk to the surface, where the redox reactions occur, over a brief distance [29]. The presence of sulfur and iron is confirmed by an EDX study of the iron sulfides' surface. in agreement with the purity of the phases observed by XRD.

3.5 X-ray photoelectron spectroscopy assay

The samples' chemical states and elemental composition were determined using X-ray photoelectron spectroscopy. As seen in Fig. 5, the XPS examination results verified that the desired catalyst comprises components like Fe and S. The presence of O was attributed to the high-resolution peak observed at 531 eV [25]. The pyrite signal at 711 eV, which dominates the Fe 2p spectra of the produced catalyst, suggests that Fe exists in Fe 2p 3/2 [30], which is significantly closer to literature values of 707.3 eV. The pyrite product being exposed to air is thought to be the cause of the disulfide formation, as indicated by the peak in the S spectra at 169 eV, which is caused by sulphates [SO_4^{2-}].

3.6 Photocatalytic activity of FeS_2

Under visible light illumination, the degradation of 2, 4-DNP organic pollutant was investigated using the photocatalytic activity of produced FeS_2. The commercially obtained FeS_2 was first subjected to harsh testing conditions, such as 0.05 g of catalyst and 10 ppm of alkaline dye solution (based on literature). The results showed a lower degradation efficiency (42%), as shown in Fig. 6a. When 2, 4-DNP was later evaluated for degradation using hydrothermally produced FeS_2, it performed better, degrading 74% of the sample in 90 minutes (Fig. 6b). The 2,4-DNP photocatalyst that was suspended in the dye solution was gathered and repeatedly cleaned with Milli Q water and then ethanol in order to assess the hydrothermally produced catalyst's repeatability. As a result, the same photocatalyst was employed once more for a continuous six cycles of dye solution degradation below comparable visible light irradiations. The produced catalyst has a remarkable capacity for degradation up to six consecutive cycles with minimal catalyst loss, according to the experiment results (Fig. 7a). A certain amount of catalyst may be lost during washes, which could account for the variations in photodegradation rate. Following an analysis of the tested composite's repeatability, it was gathered and its stability was further examined by confirming with XRD patterns that were in good agreement with newly catalyst (Fig.7b). It is concluded that the synthesized composite is a more stable photocatalyst that can be reused for six cycles in a row with minimal loss degradation rate.

3.6.1 Mechanism for 2,4-DNP degradation

Fig.8 depicted the potential photocatalysis mechanism. After the composite was first exposed to light, an electron moves from VB, where it forms holes (h^+), to CB, where it forms electrons (e^-). Together with the water molecule, the reactive species h^+ and e^- form. OH and O_2-radicals interact with dye molecules on the catalyst's surface, ultimately converting them into H_2O and CO_2 breakdown products.

$$FeS_2 + Light \longrightarrow h^+ + e^- \quad \text{Eq (2)}$$

$$H_2O + h^+ \longrightarrow {}^{\bullet}OH \quad (3)$$

$$H_2O + e^- \longrightarrow {}^{\bullet}O_2^- \quad (4)$$

$$FeS_2\ (h^+ + e^-) \longrightarrow CO_2 + H_2O \quad \text{Eq (5)}$$

4. Conclusions

This study reported on the hydrothermal preparation of metal oxide and metal sulfide (FeS2) combination. The intended 35 nm-sized composite's pure phase development was validated by the characterization analysis results. Nonetheless, under visible light irradiation, the produced composite was tested for its photocatalytic activity over the breakdown of 2,4-DNP dye solution. The created FeS_2 effectively broke down 2,4-DNP dye with a 74% degradation rate in 90 minutes; nevertheless, the ideal conditions—pH, catalyst dosage, and dye concentration—need to be investigated. pH-9, 10 ppm dye aqueous solution, and 50 mg catalyst load were shown to be sufficient for the entire 90-minute degradation of 2,4-DNP. Therefore, the current FeS_2

can be utilized to clear the contaminated water on a big scale with more efficiency and cost-effective.

Conflicts of interest

The authors declared that no conflicts of interest.

Acknowledgement

The author DA Deepthi expresses her gratitude to the Principal, St. Joseph's College for Women (A), Visakhapatnam for financial assistance through SEED fund () and the Director, Bio Enviro Chemical Solutions, Visakhapatnam for their valuable support in collaboration and characterization facilities.

References

[1] A. Ameta, R. Ameta, M. Ahuja. (2013). Photocatalytic degradation of methylene blue over ferric tungstate. Scientific Reviews & Chemical Communications. 3(3): 172-180.

[2] S.M. Botsa, K. Basavaiah. (2020). Fabrication of multifunctional TANI/Cu2O/Ag nanocomposite for environmental abatement. Scientific reports. 10(1): 14080.

[3] S.S. Patil, V.M. Shinde. (1988). Biodegradation studies of aniline and nitrobenzene in aniline plant wastewater by gas chromatography. Environmental science & technology. 22(10): 1160-1165.

[4] G.S. Sree, S.M. Botsa, B.J.M. Reddy, K.V.B. Ranjitha. (2020). Enhanced UV–Visible triggered photocatalytic degradation of Brilliant green by reduced graphene oxide based NiO and CuO ternary nanocomposite and their antimicrobial activity. Arabian Journal of Chemistry. 13(4): 5137-5150.

[5] Y.M. Slokar, A.M. Le Marechal. (1998). Methods of decoloration of textile wastewaters. Dyes and pigments. 37(4): 335-356.

[6] O. Legrini, E. Oliveros, A. Braun. (1993). Photochemical processes for water treatment. Chemical reviews. 93(2): 671-698.

[7] H.-t. Gao, Y.-y. Liu, C.-h. Ding, D.-m. Dai, G.-j. Liu. (2011). Synthesis, characterization, and theoretical study of N, S-codoped nano-TiO2 with photocatalytic activities. International Journal of Minerals, Metallurgy, and Materials. 18(5): 606-614.

[8] R. Yang, J.-h. Liu, S.-m. Li. (2011). Preparation and characterization of in-site regenerated TiO 2-ACFs photocatalyst. International Journal of Minerals, Metallurgy, and Materials. 18: 357-363.

[9] S. Xun, Z. Zhang, T. Wang, D. Jiang, H. Li. (2016). Synthesis of novel metal nanoparitcles/SnNb2O6 nanosheets plasmonic nanocomposite photocatalysts with enhanced visible-light photocatalytic activity and mechanism insight. Journal of Alloys and Compounds. 685: 647-655.

[10] S. Ahluwalia, N.T. Prakash, R. Prakash, B. Pal. (2016). Improved degradation of methyl orange dye using bio-co-catalyst Se nanoparticles impregnated ZnS photocatalyst under UV irradiation. Chemical Engineering Journal. 306: 1041-1048.

[11] P. Wang, S. Sun, X. Zhang, X. Ge, W. Lü. (2016). Efficient degradation of organic pollutants and hydrogen evolution by gC 3 N 4 using melamine as the precursor and urea as the modifier. Royal Society of Chemistry. 6(40): 33589-33598.

[12] J. Tian, Y. Leng, H. Cui, H. Liu. (2015). Hydrogenated TiO2 nanobelts as highly efficient photocatalytic organic dye degradation and hydrogen evolution photocatalyst. Journal of hazardous materials. 299: 165-173.

[13] C.H. Lai, M.Y. Lu, L.J. Chen. (2012). Metal sulfides nanostructures: synthesis, properties and applications in energy conversion and storage. Journal of materials chemistry. 22, 19–30.

[14] K. Zhang, L. Guo. (2013). Metal sulphide semiconductors for photocatalytic hydrogen production. Catalysis Science & Technology. 3(7): 1672-1690.

[15] Y. Li, Y. Hu, S. Peng, G. Lu, S. Li. (2009). Synthesis of CdS nanorods by an ethylenediamine assisted hydrothermal method for photocatalytic hydrogen evolution. The Journal of Physical Chemistry C. 113(21): 9352-9358.

[16] S. Liu, M. Li, S. Li, H. Li, L. Yan. (2013). Synthesis and adsorption/photocatalysis performance of pyrite FeS2. Applied surface science. 268: 213-217.

[17] S.K. Bhar, S. Jana, A. Mondal, N. Mukherjee. (2013). Photocatalytic degradation of organic dye on porous iron sulfide film surface. Journal of colloid and interface science. 393: 286-290.

[18] S.K. Kansal, N. Kaur, S. Singh. (2009). Photocatalytic degradation of two commercial reactive dyes in aqueous phase using nanophotocatalysts. Nanoscale research letters. 4: 709-716.

[19] A. Tian, Q. Xu, X. Shi, H. Yang, X. Xue, J. You, X. Wang, C. Dong, X. Yan, H. Zhou. (2015). Pyrite nanotube array films as an efficient photocatalyst for degradation of methylene blue and phenol. Royal Society of Chemistry. 5(77): 62724-62731.

[20] J. Puthussery, S. Seefeld, N. Berry, M. Gibbs, M. Law. (2011). Colloidal iron pyrite (FeS2) nanocrystal inks for thin-film photovoltaics. Journal of the American Chemical Society. 133(4): 716-719.

[21] M. Wang, C. Xing, K. Cao, L. Zhang, J. Liu, L. Meng. (2014). Template-directed synthesis of pyrite (FeS 2) nanorod arrays with an enhanced photoresponse. Journal of Materials Chemistry A. 2(25): 9496-9505.

[22] Y.-Y. Lin, D.-Y. Wang, H.-C. Yen, H.-L. Chen, C.-C. Chen, C.-M. Chen, C.-Y. Tang, C.-W. Chen. (2009). Extended red light harvesting in a poly (3-hexylthiophene)/iron disulfide nanocrystal hybrid solar cell. Nanotechnology. 20(40): 405207.

[23] H. Siyu, L. Xinyu, L. Q. Yu and C. Jun. (2009). Journal of Alloys and Compounds. 472, 9–12.

[24] A.M. Golsheikh, N. Huang, H. Lim, C. Chia, I. Harrison, M. Muhamad. (2013). One-pot hydrothermal synthesis and characterization of FeS2 (pyrite)/graphene nanocomposite. Chemical Engineering Journal. 218: 276-284.

[25] M. J. M. Batista, M. N. G. Cerezo, A. Kubacka, D. Tudela, M. F. Garc´ıa. (2014). ACS Catalysis. 4, 63–72.

[26] G. Lee, M. Kang. (2013). Current Applied Physics. 13, 1482–1489.

[27] B.S. Mohan, K. Ravi, R.B. Anjaneyulu, G.S. Sree, K. Basavaiah. (2019). Fe2O3/RGO nanocomposite photocatalyst: Effective degradation of 4-Nitrophenol. Physica B: Condensed Matter. 553: 190-194.

[28] M.J. Babu, S. Botsa, R.B. Anjaneyulu, C.S. Lakshmi, R. Muralikrishna. (2018). Hydrothermal assisted synthesis of FeWO4 for degradation of 2-nitrophenol under visible light illumination. International journal of scientific research in science and technology. 4(2): 417-422.

[29] S.M. Botsa, K. Basavaiah. (2019). Removal of Nitrophenols from wastewater by monoclinic CuO/RGO nanocomposite. Nanotechnology for Environmental Engineering. 4: 1-7.

[30] G. Chandrawat, J. Tripathi, A. Sharma, J. Singh, S. Tripathi, J. Chouhan. (2020). Study of structural and optical properties of FeS2 nanoparticles prepared by polyol method. Journal of Nano-and Electronic Physics. 12(2).

[31] A.M. Huerta-Flores, L.M. Torres-Martínez, D. Sánchez-Martínez, M.E. Zarazúa-Morín. (2015). SrZrO3 powders: Alternative synthesis, characterization and application as photocatalysts for hydrogen evolution from water splitting. Fuel. 158: 66-71.

[32] L. Samad, M. Cabán-Acevedo, M.J. Shearer, K. Park, R.J. Hamers, S. Jin. (2015). Direct chemical vapor deposition synthesis of phase-pure iron pyrite (FeS2) thin films. Chemistry of Materials. 27(8): 3108-3114.

[33] C.M. Eggleston, J.-J. Ehrhardt, W. Stumm. (1996). Surface structural controls on pyrite oxidation kinetics: An XPS-UPS, STM, and modeling study. American Mineralogist. 81(9-10): 1036-1056.

[34] S. Seefeld, M. Limpinsel, Y. Liu, N. Farhi, A. Weber, Y. Zhang, N. Berry, Y.J. Kwon, C.L. Perkins, J.C. Hemminger. (2013). Iron pyrite thin films synthesized from an Fe (acac) 3 ink. Journal of the American Chemical Society. 135(11): 4412-4424.